Multiparametric MRI in prostate cancer: a radiomic study on different diffusion and perfusion models

Poster No.:	C-1838
Congress:	ECR 2018
Type:	Scientific Exhibit
Authors:	S. Monti[1], M. Aiello[1], M. Inglese[1], C. T. Diomaiuti[1], A. Ragozzino[2], C. Cavaliere[1]; [1]Naples/IT, [2]Napoli/IT
Keywords:	Genital / Reproductive system male, Oncology, Pelvis, MR, MR-Diffusion/Perfusion, Image manipulation / Reconstruction, Computer Applications-Detection, diagnosis, Diagnostic procedure, Staging, Cancer, Neoplasia, Pathology
DOI:	10.1594/ecr2018/C-1838

Aims and objectives

To evaluate radiomics features extracted from T2-weighted, diffusion weighted imaging (DWI), diffusion kurtosis imaging (DKI), Toft model (TM), and shutter-speed model (SSM) perfusion maps among prostate cancer (PCa), benign prostatic hyperplasia (BPH), and benign peripheral zone (PZ). To compare the diagnostic performance of advanced prostate radiomics to PI-RADS v2 classification.

Methods and materials

40 foci of PCa, 48 BPH nodules, and 36 benign PZ from 40 patients who underwent multiparametric MRI of prostate, to eventually address a target-biopsy, were evaluated. MRI exam was performed without endorectal coil with a 3T mMR Biograph scanner. DWI was performed using 7 b-values (0-2500 s/mm^2): classical apparent diffusion coefficient (ADC) map was generated using b values up to 1500 s/mm^2; the entire range of b values was used to compute non-Gaussian diffusion coefficient (D) and deviations from normal distribution (K) maps. Dynamic contrast-enhanced magnetic resonance imaging (DCE-MRI) parameters (K^{trans}, v_e, k_{ep} [TM & SSM] and intracellular water molecular lifetime $\#_i$ [SSM]) were also determined. 2D regions of interest were manually outlined on the axial T2w that was also used as reference image to coregister other maps. 13 first-order statistical features were extracted for each map. Feature selection was performed to identify 5 features for each model. A logistic regression classifiers were used to identify features discriminating clinically significant tumors (PIRADS 4-5) from benign PZ with an intra- and inter-model approach. The area under the receiving-operating characteristic curve (AUC), the sensitivity, the specificity and the accuracy were used to evaluate the performances of models. The intermodel approach was also tested to discriminate between BPH and other groups.

Results

Identified radiomic features differentiated PCa from benign PZ. Prediction performances were higher for diffusion features (extracted for both DWI and DKI - Fig1) than for perfusion ones (extracted for both the TM and the SSM - Fig2). These differences were confirmed independently by the number of features included in the logistic model (i.e., Model order). Intermodal approach lead to logistic regression models with very high discimination performances (AUC values close to 1) with best results for sensitivity, specificity and accuracy (more than 0.995) in the models including 4, 5, and 7 features (Fig3,4). These models were also able to significantly discriminate BPH from other groups ($p<0.001$ - Fig5).

Images for this section:

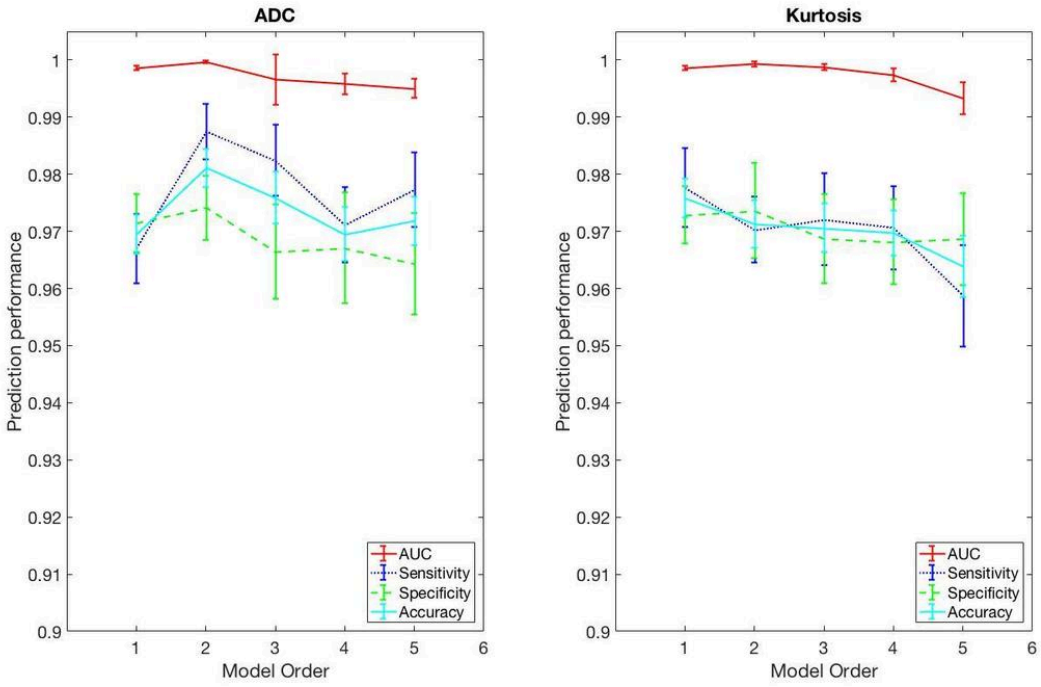

Fig. 1: Prediction performances of logistic regression models for diffusion features

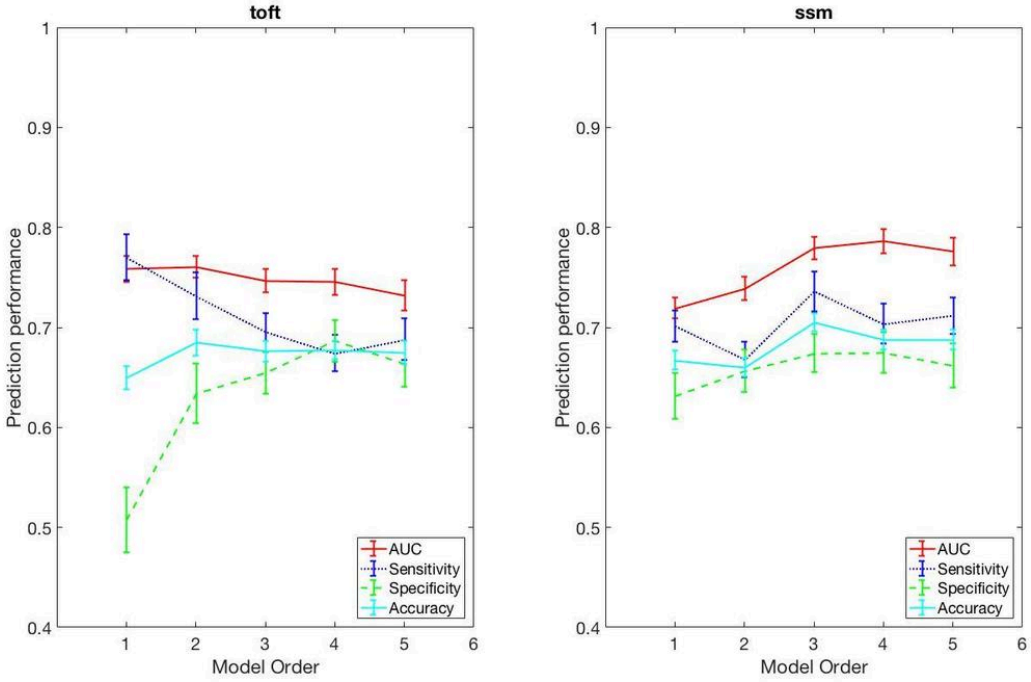

Fig. 2: Prediction performances of logistic regression models for perfusion features

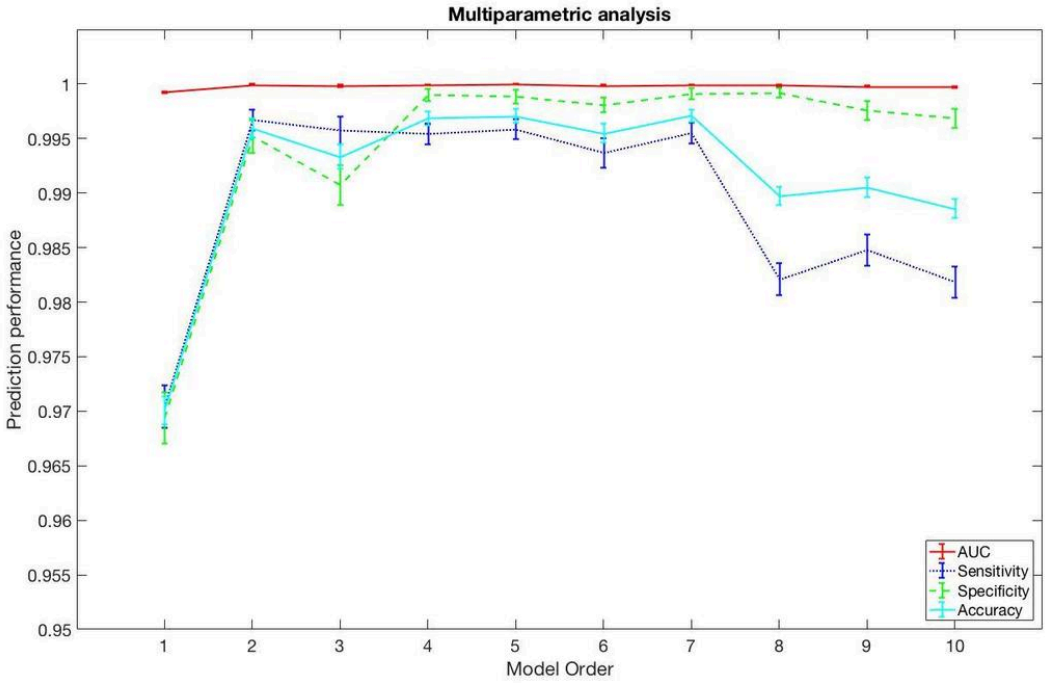

Fig. 3: Prediction performances of logistic regression analysis for intermodel approach

Model Order	Selected Features	AUC	Sensitivity	Specificity	Accuracy
1	T2w – median	0.9992	0.9704	0.9694	0.9701
2	T2w – median v_e (SSM) – uniformity	0.9999	0.9967	9.9952	0.9959
3	ADC – energy T2w – median v_e (SSM) – uniformity	0.9998	0.9958	0.9907	0.9933
4	D – maximum T2w – median T2w – skeweness ADC – skeweness	0.9999	0.9954	0.9990	0.9969
5	D – maximum T2w – median T2w – skeweness ADC – skeweness T2w – energy	0.9999	0.9958	0.9989	0.9971
6	T2w – mean v_e (SSM) – uniformity ADC – energy D – maximum k_{ep} (TM) – entropy T2w - skeweness	0.9999	0.9937	0.9981	0.9955
7	D – maximum T2w – median T2w – skeweness ADC – skeweness T2w – energy D – skeweness k^{trans} (SSM) - uniformity	0.9999	0.9955	0.9991	0.9971
8	D – maximum T2w – median T2w – skeweness ADC – skeweness T2w – energy D – skeweness k^{trans} – uniformity v_e (TM) – maximum	0.9999	0.9821	0.9992	0.9898
9	D – maximum T2w – median T2w – skeweness ADC – skeweness T2w – energy D – skeweness k^{trans} – uniformity v_e (TM) – maximum ADC – median	0.9998	0.9848	0.9976	0.9905
10	D – maximum T2w – median T2w – skeweness ADC – skeweness T2w – energy D – skeweness k^{trans} – uniformity v_e (TM) – maximum ADC – median K_{ep} (TM) – entropy	0.9997	0.9819	0.9969	0.9886

Fig. 4: AUC, Snsitivity, Specificity, and accuracy values for intermodel approach

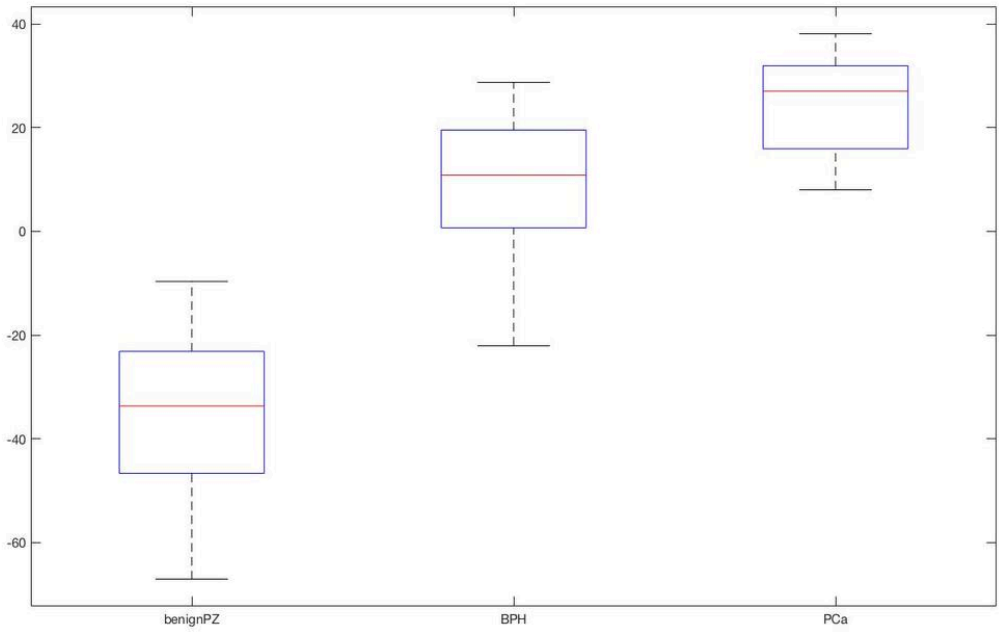

Fig. 5: Discriminating power of prediction model of order 7 between BPH and other groups.

Conclusion

Among perfusion features, parameters extracted by SSM have higher predictive performances than TM-derived.

A classifier that includes features extracted from DKI significantly improves the accuracy in cancer detection.

References

- Monti S., et al. DCE-MRI pharamacokinetic-based phenotyping of invasive ductal carcinoma: a radiomic study for prediction of histologic outcomes. Contrast Media Mol Imaging (2018).

- Incoronato M., et al. Radiogenomic analysis of oncological data: a technical survey. Int J Mol Sci. 2017;18(4).